



Dry delamination via inductive heating for direct recycling of LFP cathodes

Nino Christian^a, Andreas Flegler^a, Guinevere A. Giffin^{a,b,*} 

^a Fraunhofer R&D Center Electromobility, Fraunhofer Institute for Silicate Research, Neunerplatz 2, 97082, Würzburg, Germany

^b Institute of Inorganic Chemistry, Institute for Sustainable Chemistry & Catalysis with Boron (ICB), Julius-Maximilians-University Würzburg, Am Hubland, 97074, Würzburg, Germany

ARTICLE INFO

Keywords:

Lithium-ion battery
Direct recycling
Induction
Cathode delamination
Aqueous cathode fabrication

ABSTRACT

Sustainable recycling of lithium iron phosphate (LFP) cathodes is essential to process battery waste, thus reducing resource depletion and lowering the carbon footprint of battery production. This study introduces a contactless delamination process using high-frequency induction heating to partially decompose the water-based carboxymethyl cellulose and styrene-butadiene rubber binders in LFP electrode production scrap within a temperature range that avoids damage to the LFP. Eddy currents induced in the aluminum current collector enable localized heating at the LFP composite–foil interface, allowing clean separation without toxic solvents or high-temperature furnaces. Variation of the process parameters showed that moderate heating (~240 °C) weakens binder adhesion effectively while preserving the integrity of the LFP. Electrodes were fabricated from the recovered LFP composite and evaluated in lithium metal half cells. The best-performing recovered sample (240 °C with added conductive carbon) achieved ~96 % of the discharge capacity of a recovered sample delaminated without the inductive heat treatment. These results confirm that inductive delamination, with careful temperature control, enables the recovery of high-quality LFP composite suitable for reuse. This method avoids the use of hazardous chemicals and is compatible with roll-to-roll processing, offering a scalable and environmentally-friendly route for direct cathode recycling.

1. Introduction

The transition to electric mobility and stationary energy storage necessitates sustainable recycling approaches to manage rising material demand and waste streams. Unlike lithium nickel manganese cobalt oxide (NCM) systems, lithium iron phosphate (LFP) recycling is dependent on low-cost, high-yield recovery due to the absence of high-value elements such as nickel or cobalt [1]. Direct recycling of LFP cathodes conserves critical raw materials like lithium and phosphorus and enables the recycled cathode material to be directly integrated into cell production, which minimizes costs and environmental impact, addressing growing regulatory and ecological pressures [2–4]. Unlike end-of-life cells, production scraps, specifically those generated before electrolyte filling, are pristine in chemical composition and free from aging or electrolyte contamination [5,6]. This enables easier material recovery and reintegration into cell production, while avoiding the need for discharging, dismantling, or handling of hazardous materials.

Current delamination methods include mechanical, solvent-based, and thermal approaches [7]. Solvent-based methods, predominantly

developed for PVDF-based NCM electrodes, often rely on organic solvents [8]. While some progress has been made to reduce toxicity and flammability, the use of organic substances generally remains less sustainable due to challenges like complex recovery processes and additional emissions [8,9]. A thermal method, where the decomposition of the binder occurs at a lower temperature than that of the active material, is an alternative approach and can be made possible through high-frequency induction heating. This method has already been demonstrated for PVDF-based NCM cathodes [7,10]. In an inductive delamination method, an alternating magnetic field induces eddy currents in the conductive aluminum substrate, causing rapid surface heating due to the skin effect, which confines the induced currents to the surface region of conductive materials [11,12]. In this work, the localized thermal input partially decomposes the carboxymethyl cellulose (CMC) and styrene-butadiene rubber (SBR) binders at the LFP composite–foil interface without requiring direct contact, external heating, or additional process media, enabling a clean and selective separation of the LFP composite from the aluminum foil. By effectively concentrating thermal energy at the interface, inductive heating reduces overall

This article is part of a special issue entitled: Battery Recycling published in Journal of Power Sources Advances.

* Corresponding author. Fraunhofer R&D Center Electromobility, Fraunhofer Institute for Silicate Research, Neunerplatz 2, 97082, Würzburg, Germany.

E-mail address: guinevere.giffin@isc.fraunhofer.de (G.A. Giffin).

<https://doi.org/10.1016/j.powera.2026.100202>

Received 30 September 2025; Received in revised form 3 January 2026; Accepted 25 January 2026

Available online 30 January 2026

2666-2485/© 2026 The Authors. Published by Elsevier Ltd. This is an open access article under the CC BY license (<http://creativecommons.org/licenses/by/4.0/>).

energy consumption and processing time while preserving the morphology and composition of the cathode material, making it suitable for direct reuse in cell manufacturing [10]. The absence of harmful solvents or high-temperature furnaces drastically reduces environmental impact and mitigates the generation of secondary waste [2,3,13]. Furthermore, localized heating supports industrial scalability, particularly in roll-to-roll systems, where cathode scrap is a major waste stream [7,14,15]. This technique aligns with the principles of circular economy by minimizing emissions, maximizing material recovery, and reducing process costs. Given its compatibility with existing roll-to-roll electrode production and its potential for integration into in-line quality control and scrap recovery systems, this method represents a significant step toward sustainable, scalable, rapid, and safe battery material recycling [7].

2. Results and discussion

The thermal properties of the individual components of the LFP composite were analyzed to determine an appropriate temperature range for inductive delamination. The term 'LFP composite' refers to the materials that compose the cathode layer (without aluminum), including the active material, (remaining) binder, and conductive carbon. Fig. 1 shows the differential thermogravimetric curves for the individual cathode components. The onset temperatures were determined from the curves (Fig. S1) by calculating the intersection of the tangent at the point of maximum gradient with the baseline [16]. This mathematically-determined onset temperature is consistently higher than the initial point of decomposition and represents the temperature at which a significant decomposition process begins. A beginning oxidation, observable as weight loss, can be detected at 210 °C for CMC and at 230 °C for SBR, with respective onset temperatures of 272 °C and 296 °C. The weight loss is attributed to the combustion of organic substances. The partial oxidation of LFP (see Eq. (1) [17] for full oxidation) starts at 250 °C, resulting in a weight gain, with a calculated onset temperature of 340 °C.



The weight gain is due to oxide formation. The oxidation of C65 begins at 570 °C, indicated by a weight loss with an onset temperature of 691 °C. These data suggest a temperature range for the induction process

between 210 °C, corresponding to the beginning of binder degradation, and the onset temperature of LFP oxidation at 340 °C. Therefore, the target temperatures of 240, 270, 300, and 330 °C were selected for inductive heating, as measured during the delamination process as described in the experimental methods. It is important to note that the temperature range proposed for induction heating is based on the observed thermal behavior of LFP in this study. The onset temperature method primarily provides an estimation of thermal events and does not fully account for the nuanced differences between surface and bulk oxidation processes. Previous studies have reported surface oxidation of LFP occurring at lower temperatures [18], which underscores the limitations of the onset temperature method for assigning safe operating ranges. Despite these limitations, the specific temperatures of 240, 270, 300, and 330 °C were selected because they are sufficiently spaced to allow a clear distinction of effects between the individual temperature levels. Furthermore, these temperatures are carefully positioned within the thermal range relevant for delamination, ensuring that the process proceeds effectively above the binder degradation temperature, while avoiding temperatures at which significant bulk decomposition of LFP occurs. This deliberate selection is critical to accurately investigate the behavior within the relevant thermal range.

The cathode samples were placed in the induction field under uniform and controlled conditions. During the inductive heating process, the surface temperature of the cathodes was measured using an IR thermometer. It is important to note that the temperature at the Al-LFP composite interface may be higher than the IR surface temperature measured, as the heat during the inductive process is generated within the aluminum foil while the measurements were taken at the cathode surface. After the inductive heating process, the adhesion of the LFP composite to the current collector foil decreased significantly, resulting in partial delamination of the layers when subjected to small mechanical deformation (Fig. 2).

Z-direction adhesion tests (Fig. 3) demonstrated that the adhesion strength decreased from 930 (\pm 170) kPa for the pristine cathode to less than 350 kPa for the heated samples (350 \pm 120 kPa at 240 °C, 260 \pm 90 kPa at 270 °C, 200 \pm 120 kPa at 300 °C, and 80 \pm 30 kPa at 330 °C). Given the standard deviation of the measurements at a single temperature, there is no significant difference in adhesion between 240 °C and 300 °C. Nonetheless, a trend of decreasing adhesion strength with increasing temperature is evident. TGA of the LFP composite materials

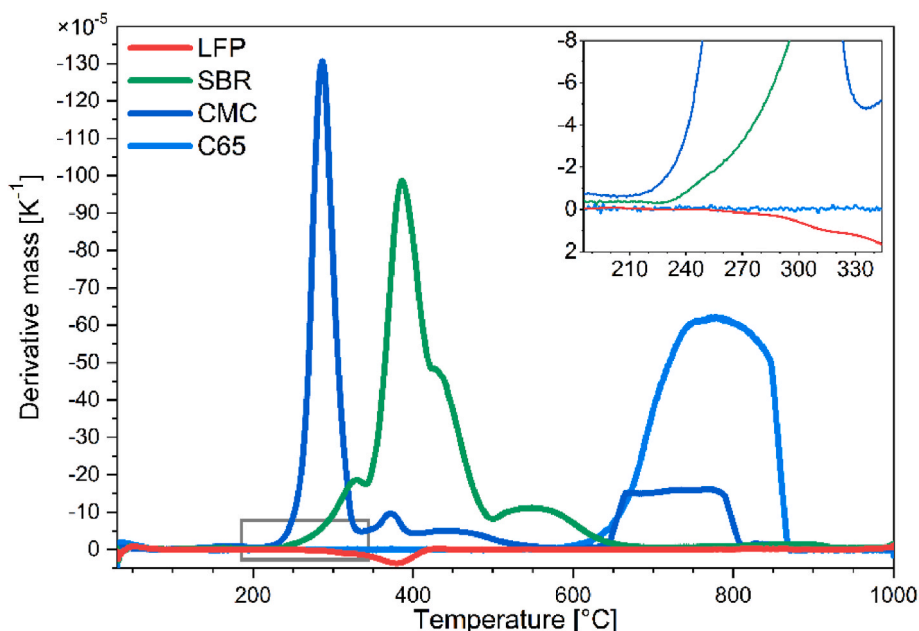


Fig. 1. Derivative thermogravimetric analysis (TGA) curves of the individual cathode components measured in dry synthetic air (N_2/O_2 , 80:20).

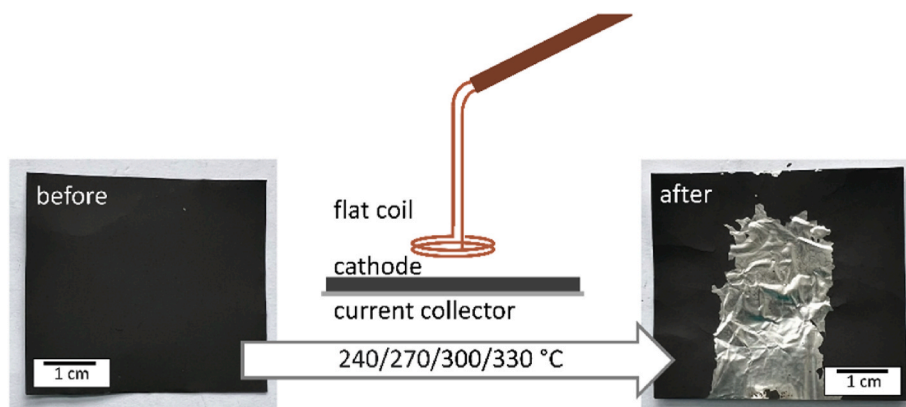


Fig. 2. Visualization of the dry delamination principle via inductive heating. Picture taken from the sample at 300 °C.

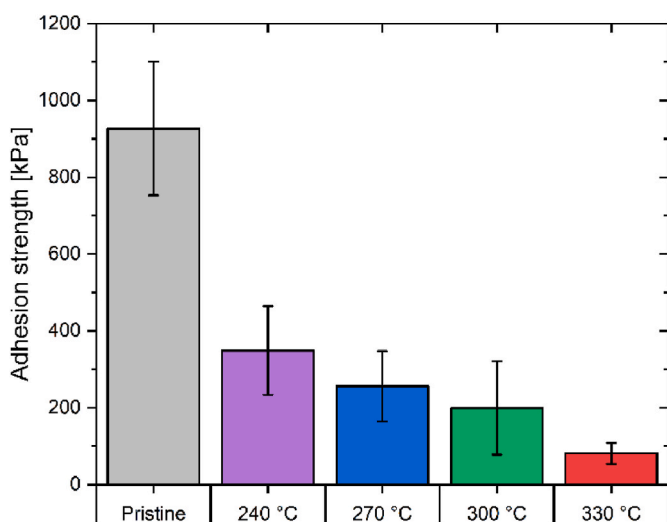


Fig. 3. Adhesion strength of the LFP composites with the aluminum current collector after inductive treatment at different temperatures and of the pristine electrode.

(Fig. S2) revealed that the mass loss of the composites decreases with increasing temperature of the inductive-delamination process. The increased mass loss suggests that there is a higher extent of binder decomposition with higher process temperatures. These findings suggest that higher process temperatures, which lead to more significant binder degradation, likely contribute to weakened adhesion between the LFP composite and aluminum foil.

The reduction in adhesion can be attributed to the partial decomposition of the binder materials and was examined using attenuated total reflection fourier transform infrared spectroscopy (ATR-IR). The spectra of the four LFP cathode components and the pristine LFP composite are shown in Fig. S3, while the edge-peeled (e.p.) and inductively-delaminated LFP composites are shown in Fig. S4. In the spectrum of the SBR binder, there is a peak at 700 cm^{-1} , which can be attributed to the out-of-plane bending mode of the aromatic C-H bonds in SBR (Fig. S5) [19,20]. This peak does not significantly overlap with features associated with the other cathode components and is the most intense peak in the ATR-IR spectrum of SBR. Furthermore, the delamination process may also be influenced by the difference in thermal expansion coefficients of the materials involved. Aluminum has a thermal expansion coefficient of $\alpha_{\text{Al}} \approx 23 \times 10^{-6}\text{ K}^{-1}$ [21], while LFP has a lower thermal expansion coefficient of $\alpha_{\text{LFP}} \approx 14 \times 10^{-6}\text{ K}^{-1}$ [22]. This mismatch in thermal expansion could induce mechanical stress at the interface during heating, potentially contributing to the separation of the layers. It

should be noted that the reported value for LFP corresponds to its bulk material properties, while the actual thermal expansion behavior of the composite may deviate due to the presence of additional components and its inherent porosity.

The quality of the LFP composite was evaluated after delamination from the current collector. The LFP was examined via XRD (Fig. S6) to assess if the bulk structure of the LFP is affected by the inductive treatment. The XRD diffraction patterns of the LFP material remain unchanged, indicating that its bulk structure and crystal structure were unaffected by the experimental conditions.

The combination of the XRD results with the ATR-IR spectra and adhesion tests suggests that the effects observed are primarily related to the decomposition of the binder and have no impact on the bulk structure of the LFP material. While only a single crystalline phase is observed in the diffraction pattern, this does not rule out the possibility of a phase transition occurring at the surface of the LFP structure. Given that the penetration depth of powder XRD extends to several micrometers, the technique lacks sensitivity to detect structural modifications confined to the nanometer-scale surface region of the material. Additionally, the SEM images (Fig. 4) show that no morphological changes occur during the inductive heating.

After separation of the LFP composite and aluminum current collector, most recovered composites contain small amounts of aluminum, which can become an issue in further processing steps and may require additional purification. To evaluate the performance of inductive delamination, the aluminum content of the LFP composite was measured via inductively coupled plasma optical emission spectroscopy (ICP-OES) and compared with results from the literature (Table 1). While there is no significant difference between edge-peeled and inductively-delaminated samples in terms of aluminum contamination, benchmarking the inductive delamination against other techniques reveals its advantages over conventional methods. Compared to literature values for sieved black mass, the inductively-delaminated LFP composite exhibits an aluminum content that is lower by one order of magnitude. Furthermore, aluminum impurity levels reported for NMC black mass obtained via electrohydraulic fragmentation (EHF) are significantly higher.

Minimizing aluminum contamination in the slurry is essential, as previous research has demonstrated that binding polymers such as CMC are highly reactive to trivalent cations. Specifically, aluminum ions can act as cationic crosslinkers, forming three-dimensional structures with CMC [25]. This crosslinking has been shown to cause significant changes in rheological properties, hinder dispersion, and lead to non-reproducible variations during the production of recovered cathodes. This effect has been observed even at low aluminum concentrations ($\sim 0.02\text{ wt}\%$), with the severity increasing with the aluminum content. Moreover, the amount of aluminum present in the recovered cathode must also be minimized in terms of cathode quality, as previous

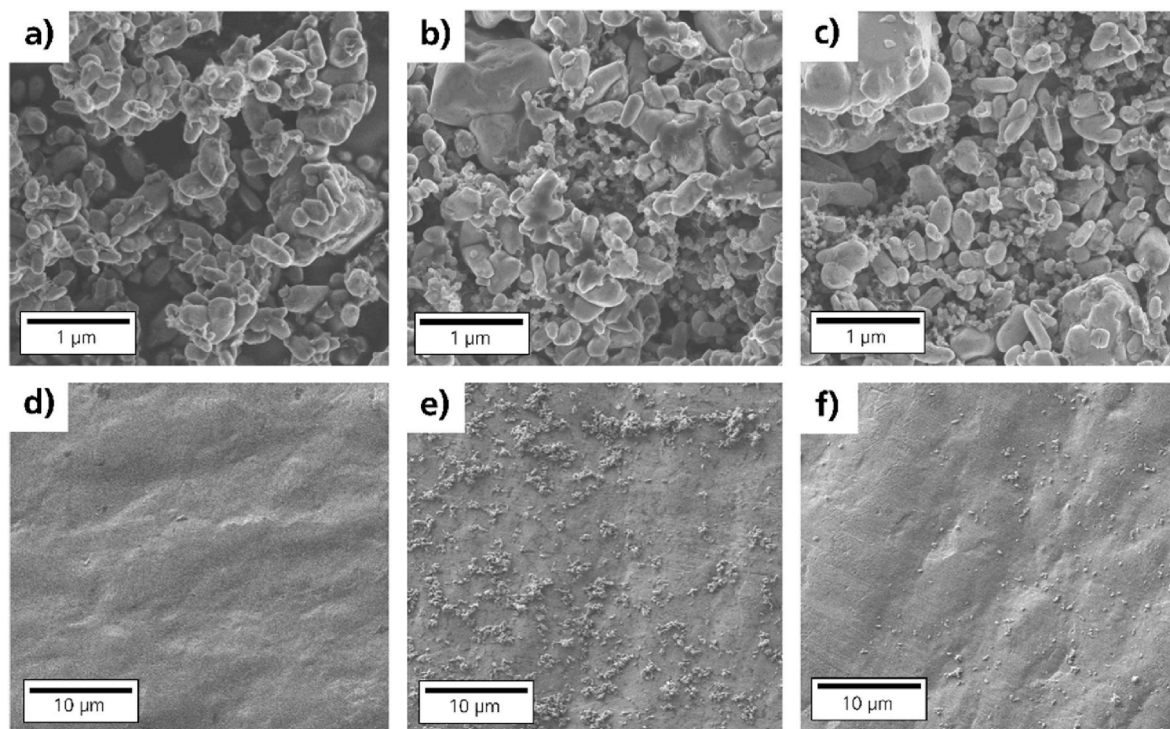


Fig. 4. SEM images of a) pristine LFP powder; b) edge-peeled LFP composite (after grinding); c) inductively-delaminated (330 °C) LFP composite (after grinding); d) pristine aluminum foil; e) aluminum foil after edge peeling; f) aluminum foil after inductive delamination (330 °C).

Table 1

Aluminum contents of recovered composites, analyzed via ICP-OES.

Sample	Al content/wt%	Source
NMC black mass from EHF	5.53	[23]
Heat-treated, sieved LFP black mass	0.59 ± 0.11	[24]
Edge-peeled LFP composite	0.0217 ± 0.0018	This work
Inductive delamination (330 °C) LFP composite	0.0225 ± 0.0020	This work

research has reported that aluminum concentrations of ~0.2 wt% in recovered cathodes can have a negative effect on battery performance [26]. In contrast, the observed contamination of ~0.02 wt% in the inductively-delaminated LFP composite lies well below this amount, demonstrating a clear advantage over conventional methods, which often result in higher levels of aluminum contamination [23,24]. This comparison highlights the potential of inductive delamination to minimize aluminum contamination, improving the quality of recovered materials and enhancing their suitability for further processing.

While the contamination of the LFP composite with aluminum is comparably low for both delamination methods, an examination of the aluminum foil surface after edge peeling reveals a significant difference in the residual LFP composite. The edge-peeled aluminum foil (Fig. 4e) exhibits visibly more adhered LFP composite than the inductively-heated foil (Fig. 4f). The SEM-EDS measurements (Fig. S7) demonstrate that the smooth areas of the foil have only minimal carbon impurities on top of the aluminum metal (which is likely also passivated by Al₂O₃ based on the oxygen peak in the EDS). The surface contamination of the inductively-delaminated Al foil is significantly less than that of edge-peeled Al foil. This demonstrates that the inductive delamination process is more effective at recovering higher-purity aluminum compared to edge peeling.

To evaluate the impact of heating and binder decomposition during delamination on the quality of the recovered material, new electrodes were prepared with the recovered LFP composites. The composites were ground by hand, redispersed in water with new CMC and SBR

binder, and coated on new Al foil (areal loading ~1.9 mAh/cm²). The recovered electrodes were integrated into half cells with a lithium metal counter electrode in a pouch cell format. These cells underwent 80 charge/discharge cycles (Fig. 5a), where the first 30 cycles included cell formation and a rate capability test (5 cycles each at C/10, C/5, C/2, 1C, 2C, and C/2). Distinct differences between the cells with the edge-peeled and the inductively-delaminated composites are evident. The recovered reference material, obtained via edge peeling (labelled as 'e.p.') exhibited only a slight capacity loss of 3 % (97 % capacity retention) compared to the pristine LFP composite cells in the first cycle after the C-rate test. Greater capacity losses were evident for the inductively-delaminated composites, where the lowest temperature (240 °C) during delamination led to a capacity retention of 85 %. The capacity losses increased dramatically with higher delamination temperatures, as seen already during the C-rate tests. The difference between the 240 °C and the higher temperature-treated samples is significant. At 270 °C, the capacity retention falls to only 18 % compared to the edge-peeled cell during the first 1C cycle after the rate test (Cycle 31). The other samples retained less than 10 % of the capacity after the rate test.

It seems that induction heating results in partial decomposition of the binders, and it is likely that decomposition products remain within the LFP composite [27]. The initial capacity of all cells in the first cycle is comparable. In addition, the overpotential during the first charge is small, which seems to imply that the decomposition products do not form an overly resistive layer. However, the overpotential increases during the first discharge cycle with higher inductive-heating temperatures of 270 °C and above (Fig. 5b), and becomes more pronounced in subsequent cycles (Fig. 5c). It is likely that the products of binder decomposition react, e.g., with the electrolyte during cycling and result in the formation of a resistive layer, which would explain the increased cell polarization. The impedance data also supports the formation of a more resistive surface layer (Fig. S8a), particularly at higher delamination temperatures. The data from the sample delaminated at 330 °C is dominated by a single large semi-circle, while the 240 °C and e.p.

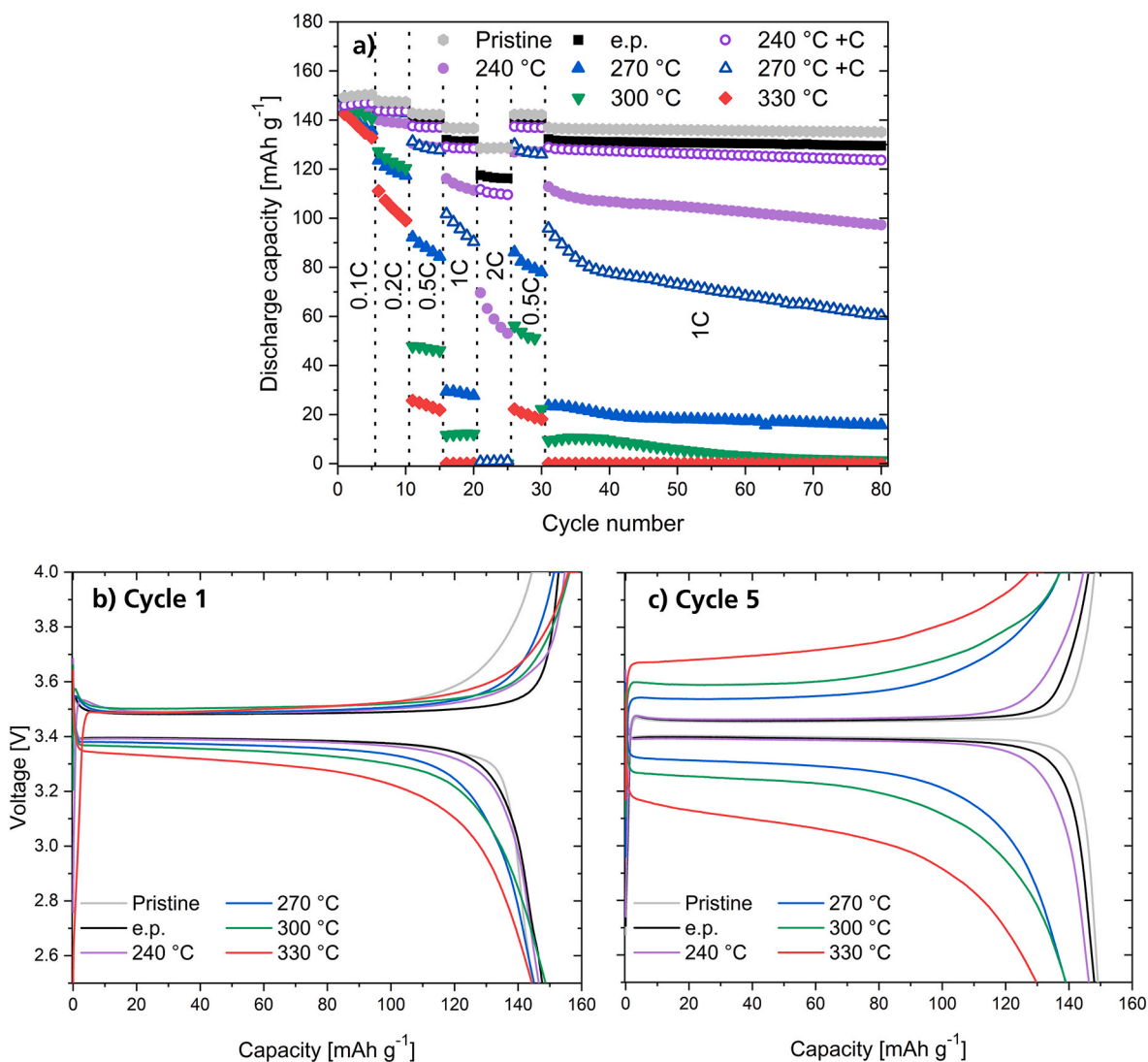


Fig. 5. Electrochemical performance of the recovered cathodes. a) Discharge capacities of the 3.5 mAh half cells with recovered cathodes. For comparison, reference cathodes (without heat treatment, but edge-peeled (e.p.) LFP composite, integrated into a new cathode) and pristine cathodes were used. Three cells per sample were cycled with five formation cycles (C/10) and a C-rate test with five cycles for each C-rate (C/5, C/2, 1C, 2C, C/2). Error bars (the standard deviation of three cells each) were excluded for better visibility. b) Voltage curves of cycle 1 and c) cycle 5.

samples show at least two semi-circles and a much smaller overall resistance. The high-frequency semi-circle typically contains contributions from cathode surface layers along with the solid-electrolyte interphase formed at the anode [28,29]. These results are also supported by the coulombic efficiencies (Fig. S8b), which are dependent on the temperature of the inductive heating process. After the first cycle, the coulombic efficiency is lower at a given C-rate with increasing temperature of the delamination process. The low coulombic efficiencies are consistent with side reactions which result in the formation of a resistive layer on the cathode. These side reactions are more pronounced with higher induction heating temperature. X-ray photoelectron spectroscopy (XPS) measurements were conducted to analyze the chemical composition at the cathode surface after cycling. Increases in the atomic percentages of carbon and oxygen and decreases in those of lithium and fluorine can be observed with increasing temperature of the delamination process in comparison to the edge-peeled sample after cycling (Table S1). This trend could be associated with a surface layer that is less rich in LiF and more rich in decomposition products originating from reactions with the electrolyte solvents [30]. The increases are more pronounced for samples subjected to higher induction heating temperatures, suggesting that the higher heating temperature forms more

binder decomposition species, which promote the formation of CEI species by decomposition of the electrolyte. Additionally, the beginning LFP oxidation during delamination, especially for the 300 °C and 330 °C samples may also contribute to the lower capacity retention.

These explanations do not sufficiently address the low capacity retention of the inductively-delaminated sample heated to 240 °C, particularly during the C-rate test. The significant capacity drop in the 2C cycles suggests a reduced electronic conductivity within the LFP composite [31]. This hypothesis was addressed by adding conductive carbon (C65) to the slurry (labelled as '240 °C + C' and '270 °C + C') during recovered electrode processing. The capacity retention of these cells was 97 % and 72 %, respectively, of that of the reference cells in the first cycle after the rate test. This is a significant improvement compared to the recovered LFP composites without additional conductive carbon. Nonetheless, differences between the 240 °C + C and 270 °C + C remain. While there are only minor increases in the overpotential of the 240 °C + C cells (mostly at the end of charge and discharge, where mass transport effects dominate), increased polarization is evident with the 270 °C + C LFP composites even in the first cycle (Fig. S9). These results suggest that there are two effects at play: 1) the reduced electronic conductivity of the composite; and 2) detrimental species resulting from

binder decomposition, most notably at 270 °C and above, which then cause side reactions within the cell at the cathode-electrolyte interface.

The first effect can be mostly compensated for through the use of additional conductive carbon. The recycling/reuse process, which is not optimized, likely contributes to the loss of conductivity. The recovered LFP composites were manually ground with a mortar and pestle. Nonetheless, aggregates were evident in the composite, which could not be redispersed during slurry preparation. These agglomerates may result in isolated regions with poor electronic contact and/or reduced mass transport.

3. Conclusion

The successful inductive delamination of water-processed LFP cathodes and the subsequent reuse of the recovered LFP composite in water-based cathodes were demonstrated. The study highlights that a significant dependence on the heating temperature, with lower temperatures (240 °C) yielding the best cell performance with recovered LFP composite. Although higher temperatures (330 °C) further reduce the adhesion to the current collector due to further decomposition of the binder, the decomposition products are assumed to negatively impact the electrochemical performance. The presence of potential decomposition products likely contributes to the increased overpotential and impedance, with this effect becoming more pronounced during galvanostatic cycling. This behavior can likely be attributed to reactions occurring between the binder decomposition products and the electrolyte, leading to the formation of a resistive layer that contribute to the increased cell polarization. Further improvements in the electrochemical performance of the recovered LFP composites could be obtained through the addition of conductive carbon, emphasizing that a portion of the performance limitation is related to conductivity issues within the cathode, and highlighting the need for optimization of the process steps after delamination.

Inductive heating has proved to be a highly efficient and sustainable method for delaminating electrode materials. It eliminates the need for solvents, allows for a rapid process, and enables localized and precise heating that minimizes energy consumption. These advantages align well with the goals of green and scalable battery recycling processes.

4. Experimental section

Electrode preparation: An aqueous slurry consisting of 88 wt% carbon-coated lithium iron phosphate active material (LFP, Lot number: 2298 GF 195, Johnson Matthey Battery Materials GmbH, Germany), 2 wt% carboxymethyl cellulose (CMC, MW ~250,000 g/mol, degree of substitution 0.9, Sigma Aldrich Chemie GmbH), and 5 wt% styrene butadiene rubber (SBR, Lot number: LR108P-211215, 15 wt% dispersion, Targray) as binders and 5 wt% Super C65 (C-ENERGY™, Imerys S. A.) as conductive carbon was prepared as follows. CMC was dissolved in deionized water overnight. LFP and C65 were dry mixed and added to the CMC solution. The resultant slurry was mixed for 2 h using a SpeedMixer (CAS 400.1 VAC-P, Hauschild GmbH & Co. KG). The SBR was added during the last 10 min. The total amount of water in the final slurry was 120 wt% of the solid content. The slurry was coated using the doctor blade method onto 20 µm thick aluminum foil (Korff AG, Switzerland). The coating was dried in an oven at 80 °C for 2 h. The dried LFP electrode was then calendered to a porosity of 40 %. Discs with a diameter of 16 mm were punched from the layer and dried under vacuum for 12 h and 110 °C. The areal capacity of the cathodes was in the range of 1.7–2.0 mAh cm⁻².

Inductive delamination process: The LFP electrode was cut into squares measuring 3.5 cm × 3.5 cm and was positioned centrally at a distance of 1.0 cm from the coil. The electrode samples were exposed to a high-frequency induction field in ambient air. A Sinus 102 (Himmelwerk, Germany) with 10 kW, 2 MHz, a high-frequency voltage of 440 V, and a capacitance of 100 nF was used. A specially-designed HG7527 coil

(Himmelwerk, Germany), displayed in Fig. S10 with a frequency of 1.754 MHz and an inductance of 7.11 × 10⁻⁸ H, was used. The temperature was measured during the process using an infrared thermometer (CTlaser LT, Optris GmbH & Co. KG) and maintained at 240/270/300/330 °C ± 10 °C for 50 s. The IR thermometer was aimed at the cathode layer surface. An emissivity of 0.9 was set, which is a common value for black, non-reflective and non-metallic surfaces [32]. The delaminated LFP composite was ground into a fine powder using a mortar and pestle. A mechanically-delaminated LFP composite, which served as a reference, was detached from the aluminum foil via edge peeling and ground into a powder with a mortar and pestle.

Electrode preparation with recovered LFP composites: The recovered LFP composites, which were already ground, were processed into a slurry using fresh CMC, SBR, and deionized water, as described in the 'Electrode preparation' section above. The fresh binders accounted for 4.1 % of the solid slurry components (0.5 % CMC: 3.6 % SBR). The electrodes contain only recovered LFP and are not blended with fresh material. Areal capacities of the cathodes ranged from 1.7 to 2.0 mAh cm⁻². In addition, LFP cathodes were fabricated as described above, but 50 % additional C65, relative to the initial amount, was dry mixed with the LFP composite.

Electrochemical testing: Cells were assembled from the recovered electrodes and a lithium metal counter electrode (Gelon Lib Group Co., Ltd., China), a Celgard 2500 separator (Celgard, USA), and 200 µL of a 1 mol/L LiPF₆ solution in EC/DMC 1:1 wt%/wt% with 5 % FEC electrolyte (E-Lyte Innovations GmbH, Germany) in a pouch cell format. The surface of the lithium metal was scraped using a ceramic knife. The cells were prepared in an argon atmosphere in a glovebox (GS-Glovebox, O₂ < 1.0 ppm, H₂O < 0.1 ppm). The cells were cycled between 2.5 V and 4.0 V on an electrochemical workstation (Maccor, Series 4000, Maccor Inc., USA) at 25 °C (IPP260, Memmert GmbH + Co. KG). The cells were charged in CCCV mode, with a current limitation of C/20 during the CV step, and discharged in CC mode. Cell formation was performed with five cycles at C/10, followed by a C-rate test consisting of five cycles at C-rates of C/5, C/2, 1C, 2C, and again C/2, followed by 50 cycles at 1C.

EIS measurements: Electrochemical impedance spectroscopy (EIS) measurements of the half cells were performed using a VMP300 galvanostat/potentiostat (BioLogic GmbH, France). The cells were cycled five times at a rate of C/10 as a formation process in the voltage window of 2.5 V–4.0 V. EIS measurements were performed at a 50 % SOC (defined as half of the total charge capacity) after a 6 h rest period. Impedance spectra were recorded using an amplitude of 5 mV and a frequency range from 10 mHz to 6 MHz.

Characterization methods: Thermogravimetric analysis of the components of the LFP composite were conducted using a STA 449 C Jupiter (Netzsch Group, Germany) with a heating rate of 10 K/min in a temperature range from 30 °C to 1000 °C in dry synthetic air (N₂/O₂ 80:20). For ICP-OES measurements, the LFP composites were digested in aqua regia, the residue was filtered, and the filtrate was measured using a Vista Pro spectrometer (Varian Inc., USA). Attenuated total reflection fourier transform infrared spectroscopy spectra of the LFP composites were acquired with an Alpha ATR-IR spectrometer (Bruker Optik GmbH, Germany) with a germanium crystal. Powder XRD measurements of the ground LFP composite and the LFP reference were performed using a SmartLab diffractometer (Rigaku Corporation) with Cu Kα radiation (λ ≈ 1.5418 Å), operating in a 2θ range of 10–80° at a scan rate of 0.5°/min. Images of the ground LFP composites and the aluminum foils were acquired using a ZEISS Ultra 55 scanning electron microscope (Carl Zeiss Microscopy GmbH, Germany) operated at an acceleration voltage of 2 kV. For the LFP composites, an InLens secondary electron detector was used to enhance surface detail and resolution. To improve topographical contrast, images of the aluminum foils were obtained using the SE2 secondary electron detector. The EDS measurements were conducted with an EDS detector (EDAX, LLC, USA). XPS measurements were conducted using an S-Probe X-ray photoelectron spectrometer (Surface Science Instruments) with an Al-Kα monochromatic X-ray source. The

spectra were calibrated to the C 1s peak at 284.6 eV.

Z-Direction Adhesion Test: The adhesion strength of the inductively-heated electrode was tested using an AllroundLine Z100 universal testing machine (ZwickRoell GmbH & Co. KG, Germany). During the measurement, two sample mounts, each with a diameter of 11.75 mm, were covered with double-sided adhesive tape (tesa 05969, tesa, Germany), with the aluminum side of the cathode attached to one of the mounts. The mounts were pressed together with a force of 600 kPa for 30 s. Afterwards, the mounts were pulled apart at a speed of 100 mm/min, and the force until fracture was recorded [33]. The values given are the average of ten individual measurements.

CRedit authorship contribution statement

Nino Christian: Writing – review & editing, Writing – original draft, Visualization, Validation, Methodology, Investigation, Conceptualization. **Andreas Flegler:** Writing – review & editing, Supervision, Resources, Methodology, Funding acquisition, Conceptualization. **Guinevere A. Giffin:** Writing – review & editing, Visualization, Supervision, Methodology, Conceptualization.

Declaration of competing interest

The authors declare the following financial interests/personal relationships which may be considered as potential competing interests: "Given her role as executive guest editor of the Special Issue: Battery Recycling, Guinevere A. Giffin had no involvement in the peer review of this article and had no access to information regarding its peer review. Full responsibility for the editorial process for this article was delegated to another journal editor." If there are other authors, they declare that they have no known competing financial interests or personal relationships that could have appeared to influence the work reported in this paper.

Acknowledgements

The authors gratefully acknowledge the invaluable assistance of Johannes Röder for sample preparations, Franziska Stahl for cell assembly, Richard Olsowski for TGA and XRD measurements, Nadja Keidel for ICP-OES analyses, Werner Stracke for SEM measurements, Kirsten Langenbrink for XPS measurements and Bastian Fett for providing feedback on the manuscript. Their expertise and support were crucial to the successful completion of this work. This research was financially supported by the German Federal Ministry of Research, Technology and Space through the AdRecBat project (Grant Agreement no. 03XP0518B).

Appendix A. Supplementary data

Supplementary data to this article can be found online at <https://doi.org/10.1016/j.powera.2026.100202>.

[org/10.1016/j.powera.2026.100202](https://doi.org/10.1016/j.powera.2026.100202).

Data availability

Data will be made available on request.

References

- [1] S. Kumawat, D. Singh, A. Saini, *Mater. Manuf. Process.* 38 (2023) 135.
- [2] C. Aichberger, G. Jungmeier, *Energies*. 13 (2020) 6345.
- [3] L. Gaines, Q. Dai, J.T. Vaughey, S. Gillard, *Recycling*. 6 (2021) 31.
- [4] X. Lin, W. Meng, M. Yu, Z. Yang, Q. Luo, Z. Rao, T. Zhang, Y. Cao, *Front. Energy Res.* 12 (2024).
- [5] L.E. Sita, R. Sommerville, G. Alsofi, W. Da Lima Silva, D. Gastol, J. Scarmio, E. Kendrick, *Batter. Supercaps.* 8 (2024) e202400536.
- [6] C. Hanisch, J.-H. Schünemann, J. Diekmann, B. Westphal, T. Loellhoeffel, P. F. Prziwara, W. Haselrieder, A. Kwade, *ECS Trans.* 64 (2015) 131.
- [7] M. Wagner, D. Griebel, M. Hiller, A. Kwade, *J. Clean. Prod.* 428 (2023) 139338.
- [8] O. Buken, K. Mancini, A. Sarkar, *RSC Adv.* 11 (2021) 27356.
- [9] Y. Bai, R. Essehli, C.J. Jafta, K.M. Livingston, I. Belharouak, *ACS Sustainable Chem. Eng.* 9 (2021) 6048.
- [10] M. Wagner, D. Griebel, M. Hiller, A. Kwade, *J. Electrochem. Soc.* 172 (2025) 10509.
- [11] Y. Tian, L. Wang, G. Anyasodor, Z. Xu, Y. Qin, *Manuf. Rev.* 6 (2019) 17.
- [12] A. Gariépy, G. D'Amours, *Eng. Proc.* 43 (2023) 26.
- [13] X. Zhong, W. Liu, J. Han, F. Jiao, W. Qin, T. Liu, C. Zhao, *Waste Manage. (Tucson, Ariz.)* 89 (2019) 83.
- [14] M.-W. von Horstig, A. Schoo, T. Loellhoeffel, J.K. Mayer, A. Kwade, *Energy Technol.* 10 (2022) 2200689.
- [15] R. Kollack, R. Veit, M. Merklein, J. Lechler, M. Geiger, *CIRP Ann. Manuf. Technol.* 58 (2009) 275.
- [16] M.S. Egger, M. Sigl, R. Saf, H. Amenitsch, A. Torvisco, T. Rath, G. Trimmel, *J. Mater. Chem. C* (2025), <https://doi.org/10.1039/D5TC01096A>. *Advance Article*.
- [17] X. Xia, Z. Wang, L. Chen, *Electrochem. Commun.* 10 (2008) 1442.
- [18] S. Hamelet, P. Gibot, M. Casas-Cabanas, D. Bonnin, C.P. Grey, J. Cabana, J.-B. Leriche, J. Rodriguez-Carvajal, M. Courty, S. Lévassieur, et al., *J. Mater. Chem.* 19 (2009) 3979.
- [19] J.B. Azevedo, L.M.S. Murakami, A.C. Ferreira, M.F. Diniz, L.M. Silva, R.d.C. L. Dutra, *Polímeros* 28 (2018) 440.
- [20] M.J. Fernández-Berridi, N. González, A. Mugica, C. Bernicot, *Thermochim. Acta* 444 (2006) 65.
- [21] D.U. Furrer, S.L. Semiatin (Eds.), *Fundamentals of Modeling for Metals Processing*, ASM International, 2009.
- [22] M. Bertrand, S. Rousselot, D. Aymé-Perrot, M. Dollé, *Mater. Adv.* 2 (2021) 2989.
- [23] J. Öhl, D. Horn, J. Zimmermann, R. Stauber, O. Gutfleisch, *Mater. Sci. Forum* 959 (2019) 74.
- [24] O. Renier, A. Pellini, J. Spooren, *Batteries* 9 (2023) 589.
- [25] Y. Liu, Y. Chen, Y. Zhao, Z. Tong, S. Chen, *Bioresources* 10 (2015).
- [26] H. Yu, D. Zhao, K. Chen, M. Huang, H. Yang, L. Yang, Z. Wang, L. Chen, X. Ding, H. Lv, et al., *Resour. Conserv. Recycl.* 223 (2025) 108523.
- [27] D. Kessen, C. Peschel, M. Winter, S. Wiemers-Meyer, S. Nowak, *Adv. Mater. Technol.* (2025), <https://doi.org/10.1002/admt.202501394>. *Advance Article*.
- [28] S. Kiani, H. Gharibi, S. Javadian, M. Zhiani, H. Kashani, *Appl. Surf. Sci.* 633 (2023) 157638.
- [29] W. Choi, H.-C. Shin, J.M. Kim, J.-Y. Choi, W.-S. Yoon, *J. Electrochem. Sci. Technol.* 11 (2020) 1.
- [30] M.D. Bouguern, A.K. M R, K. Zaghbi, *J. Power Sources* 623 (2024) 235457.
- [31] C. Wang, J. Hong, *Electrochem. Solid State Lett.* 10 (2007) A65.
- [32] S.G. Yousef, P. Sperfeld, J. Metzendorf, *Metrologia* 37 (2000) 365.
- [33] W. Haselrieder, B. Westphal, H. Bockholt, A. Diener, S. Höft, A. Kwade, *Int. J. Adhesion Adhes.* 60 (2015) 1.